

Location of Calcium Within *Bacillus* Spores by Electron Probe X-Ray Microanalysis¹

RENÉ SCHERRER AND PHILIPP GERHARDT

Department of Microbiology and Public Health, Michigan State University, East Lansing, Michigan 48823

Received for publication 16 June 1972

Spectroscopic microanalysis of the element-characteristic X rays produced by a scanning electron microprobe was employed to detect calcium and carbon in both intact and thin-sectioned spores of *Bacillus cereus* T and *B. megaterium* QM B1551. Linear scan profiles and multilineal scan images of the X-ray emissions for calcium ($\text{Ca}_{K\alpha}$) were compared with those for carbon ($\text{C}_{K\alpha}$) as an index of mass. Location was accomplished by stereological comparisons with secondary electron images and conventional transmission electron micrographs. Although the elements could be detected at the attogram level theoretically, spatial resolution was limited to ~500 to 1,000 nm in an intact spore, e.g., by the primary electron beam diameter, the electron-excited spore microvolume, and the type of specimen support. The resolution was improved to ~100 to 200 nm by use of thin-sectioned spores, with precautions to prevent calcium leakage from the specimen during preparations. In both intact and sectioned spores, calcium was distributed throughout the spore, similarly to carbon, and concentrated mainly in a central region corresponding to the spore protoplast.

Heat resistance and other extraordinary physiological properties of the dormant bacterial spore seem related a priori to unique chemical constituents. Foremost among these in conspicuously high concentration are calcium and dipicolinic acid (DPA), which are released rapidly upon spore germination into the heat-susceptible state. An extensive literature on the subject was reviewed in a recent book (6).

The role of Ca in the cryptic mechanism of thermoresistance might be suggested if the location of Ca within the spore structure were known. Direct efforts to locate Ca heretofore have been unsuccessful because of reliance on disintegration of the spore and isolation of structural components, which liberate and possibly redistribute the element. What has been needed is a physical probe that detects the element *in situ*, together with a means for correlating the chemical determination with the spatial location.

The electron probe X-ray microanalyzer has been successfully applied for both ultramicro-detection and location of elements in higher

plant and animal tissues and cells (1, 4, 7). Furthermore, Carroll used the method with bacteria, demonstrating the presence of Ca as well as potassium, phosphorus, and silicon in the X-ray spectrum of a single spore of *Bacillus megaterium* (5). However, the location of elements within bacterial cells has not been accomplished because their size approximates the usual resolution limits of the method.

The principles of electron probe X-ray microanalysis may be summarized as follows. The electron beam in a special scanning electron microscope is focused on, penetrates, and ionizes the specimen. The cross-sectional area of the excited microvolume in the specimen, and therefore the spatial resolution of the method, depends on the diameter and energy of the electron beam and on the composition and density of the specimen and its support. The excited microvolume in a thick specimen is of greater diameter than the electron beam, but in a thin specimen the diameters are about the same. X rays are generated within the excited volume, and chemical elements can be detected by spectrographic analysis of the emitted X rays, usually by means of diffractive spectrometers. Increased sensitivity in detection can be accomplished by increasing the energy of the electron beam and thereby

¹ Article no. 5876 from the Michigan Agricultural Experiment Station. A preliminary report was presented at the 70th Annual Meeting of the American Society for Microbiology, 26 April to 1 May 1970.

the intensity of the emitted X rays. A dense mounting material backscatters electrons and thereby also enhances sensitivity, but reduces spatial resolution by increasing the excited microvolume in the specimen. The scanning mechanism of the electron probe allows a specimen to be analyzed linearly (in either a continuous or discontinuous mode) for a profile, or multilinearly for an image of the emitted X rays. The impact of the electron beam upon the specimen and its support backscatters some of the primary electrons, but also produces secondary electrons of lower energy. These electronic events are recorded on oscilloscopes and are used for studying the size, shape, and surface of the specimen. Ionization of the specimen produces a variation in the electric potential, or sample current, which is recorded in the same way.

Characteristics of the profile of Ca-specific X rays, which results as the electron microprobe beam is scanned across a spore, should depend on where the Ca is located. Some stereological predictions are diagrammed in Fig. 1 for both an intact and a sectioned spore. The first three pairs of X-ray profiles depict the results anticipated if Ca were located in only one of the three major structural regions of the spore, with the assumption that mass is distributed equally. The last pair of profiles

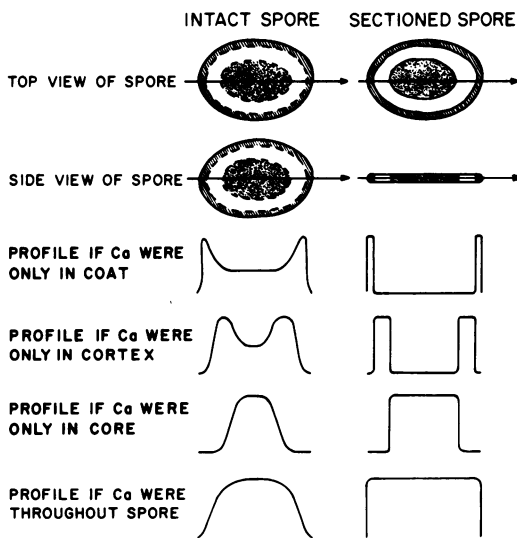


FIG. 1. Stereological predictions of normalized X-ray emission profiles for calcium in an intact spore (left column) and a sectioned one (right column), depending on the location of the element in all or only one of the three major structural regions. The relative positions of the microprobe scan are indicated by the arrows.

shows the results if Ca were distributed uniformly throughout the spore structure.

By application of the above principles, it appeared possible that the resolution of electron probe X-ray microanalysis might be improved sufficiently, and the technique coupled with conventional transmission electron microscopy, to enable location of Ca within at least the major structural regions of a dormant spore. *B. cereus* T and *B. megaterium* QM B1551 spores were chosen because of their extensive use as models and the detailed knowledge of their fine structure. Profiles from the electron microprobe were correlated with images obtained from an electron microscope, and the X-ray emissions from Ca were compared with those from carbon as an index of cell mass. Altogether, it was revealed that calcium is distributed similarly to carbon throughout the spore but is concentrated mainly in the region of the spore protoplast.

MATERIALS AND METHODS

Cell preparations. Cells of *B. cereus* T and *B. megaterium* QM B1551 were cultured and their spores were prepared as described previously (2, 10).

Calcium-labeled spores were prepared by the addition of $^{45}\text{CaCl}_2$ (specific activity 10.6 mCi/mg; New England Nuclear Corp.), in amounts of 0.02 $\mu\text{Ci/ml}$, to the sporulation media. The final specific activity therefore was 0.022 Ci/mole. Radioactivity was assayed by the use of a scintillation gel (Insta-gel, Packard Instruments Co.) and measurement with a liquid scintillation spectrometer (Mark I, Nuclear-Chicago Corp.).

Preparation of thin sections. Spores were fixed, prestained with uranyl acetate, dehydrated, and embedded according to either the Ryter-Kellenberger (8) or the Luft (9) technique, but with CaCl_2 omitted from the buffers used for fixation and washing. The embedded spores were sectioned in an LKB ultramicrotome with either a glass or a diamond knife. Section thickness was estimated by the Peachey (12) scale. The sections were allowed either to float onto a water-filled trough in the usual manner, or were collected individually directly from the edge of the knife to prevent the loss of Ca. They were then positioned on either a microprobe support or an uncoated, nickel, 200-mesh London finder grid (Maxtaform, Ernest F. Fullam, Inc.).

Microincineration. A droplet of spore suspension was allowed to dry on a stainless-steel, 200-mesh electron microscope grid which had been coated with a silicon monoxide layer as described by Thomas (14, 15). The specimen was then ashed in a muffle furnace at 600 C for 30 or 60 min.

Reference materials. Polished graphite specimens (Applied Research Laboratories) and polystyrene latex microspheres (Dow Chemical Co.), dried on quartz slides, were used as reference substances for carbon. The sesquihydrate of CaDPA , prepared

according to Strahs and Dickerson (13), was used as a calcium reference.

Specimen preparation for microprobe analysis. The specimens were dried onto polished carbon or aluminum discs, or quartz slides, and made conductive by coating lightly and uniformly with carbon in a vacuum evaporator with a rotating and tilting table. Thickness of the carbon layer was determined as described by Thomas (15). When a specimen was to be mounted on an electron microscope grid, the grid was positioned over a hole in an aluminum microprobe support.

Instruments. A model EMX-SM electron microprobe (Applied Research Laboratories) was employed. The electron optical components had been modified to produce an electron beam as little as 100 nm in diameter, as determined from a gold-tin interface (4). The instrument included facilities for optical microscopy, pulse-height analyzers, display oscilloscopes, and strip-chart recorders. Three diffractive spectrometers (Rowland circle of 4 inches) were each positioned at an angle of 52° to the specimen plane. Lithium fluoride crystals were used for the diffraction of Ca-specific X rays and lead stearate pseudocrystals, for that of C-specific X rays. Only the most intense emissions, the so-called K_{α} lines, were analyzed. No attempt was made to separate the $K_{\alpha 1}$ and $K_{\alpha 2}$ lines. Operational specifications for the microprobe, which varied somewhat with each determination, are indicated in the table and figure legends.

Transmission electron microscopy was accomplished by use of a Philips model EM 300 instrument operated at 80 kv, with conventional preparational and photographic procedures.

RESULTS

Reference comparisons. To optimize the instrumental conditions and exclude the possibility of interference by other chemical elements, the X-ray emission spectra of Ca and C in spores were compared with those in reference substances. The electron beam was focused on the center of the sample and checked by optical microscope and secondary electron images, and the spectrometer settings were varied.

The results (Fig. 2) indicated that the K_{α} lines for Ca ($Ca_{K_{\alpha}}$) in a spore had the same peak wavelength (0.3356 nm) as those in CaDPA. Calcium (atomic number = 20) has a complex X-ray emission spectrum, but the $Ca_{K_{\alpha}}$ peak from a spore was much broader and less intensive than that from CaDPA under the same experimental conditions. Compiled data on X-ray emission spectra (3) indicate that only bismuth may interfere with $Ca_{K_{\alpha}}$ lines, and bismuth was not detected in the spores.

Carbon (atomic number = 6) has a relatively simple X-ray emission spectrum. The $C_{K_{\alpha}}$

lines from a spore were much less intense than those from graphite or latex. The peak wavelength of the $C_{K_{\alpha}}$ lines in a spore (4.47 nm) was not exactly the same as in the reference substances. This anomaly is observed in elements of low atomic number and is explained by the involvement of K-shell electrons in bonding phenomena (4, 7).

The X-ray intensities from Ca and C in an intact spore were compared with those in an ashed spore and in CaDPA, with two types of specimen support (Table 1). Spores and CaDPA crystals both were remarkably stable under the electron beam for up to 30 min. However, the X-ray intensities from both Ca and C in a spore were much lower than those in CaDPA. Destruction of the spore organic matrix by microincineration abolished the C and enhanced the Ca X-ray intensity. The nature of the specimen support played an important role: a spore placed on a thick slide of quartz emitted X rays of much higher intensities than one on a thin layer of silicon monoxide.

To illustrate the continuous linear scanning mode of the microprobe, polystyrene latex microspheres of different sizes were selected as reference objects. In this mode, the focused electron beam traverses once across a specimen, and the element-specific X-ray intensity is continuously recorded as a function of the scanning distance. Latex microspheres were selected because of their spherical conformation, uniform composition, density of 1.05 g/cm³, and calibrated size. As shown in Fig. 3, the $C_{K_{\alpha}}$ intensity depended on the microsphere mass excited by the primary electron beam as a function of the scanning distance, but the profile deviated from the exact shape of a parabola. The scanned diameter of the microsphere was greater than actual because of the addition of the electron beam diameter to the real diameter of the microsphere. When the microsphere diameter approximated the spatial resolution of the microprobe, the resulting profile became ill-defined (Fig. 3A).

Orientation profiles then were obtained for spores in various positions relative to the scan. A continuous linear differential scan through a series of *B. cereus* spores is depicted in Fig. 4. As the electron beam traversed through a spore, the $C_{K_{\alpha}}$ and $Ca_{K_{\alpha}}$ intensities (Fig. 4C) increased approximately in proportion, but to extents depending on the relative positions of the spores (Fig. 4A). For example, a scan longitudinally through the center of a spore resulted in a profile with a higher intensity and a wider base than one transversely off center. The

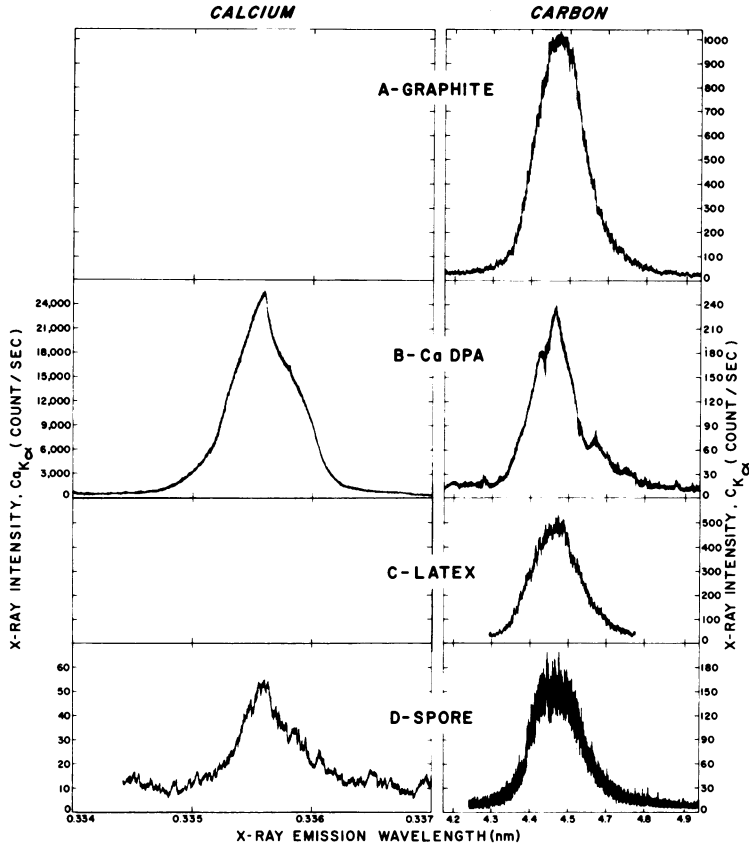


FIG. 2. X-ray emission spectra for $C_{K\alpha}$ and $Ca_{K\alpha}$ in (A) polished graphite (A), a calcium dipicolinate sesquihydrate crystal (B), a polystyrene latex sphere of diameter 1.81 μm (C), and a *B. cereus* spore (D). Microprobe specifications: 15-kv acceleration potential, 210-nm beam diameter, 25-namp sample current.

TABLE 1. Static microprobe analysis^a of $Ca_{K\alpha}$ and $C_{K\alpha}$ intensities from CaDPA and from intact and ashed spores of *B. cereus* mounted on two types of support

Specimen ^b	Support	Net X-ray intensity (counts/min) ^c	
		$C_{K\alpha}$	$Ca_{K\alpha}$
CaDPA	Quartz slide	15,704	123,156
Intact spore	Quartz slide	12,000	2,820
Intact spore	SiO layer	3,618	606
Ashed spore ^d	SiO layer	0	85,398

^a Microprobe specifications: 15-kv acceleration potential, 200-nm beam diameter, 20-namp sample current; point analysis of the CaDPA crystal surface at an angle normal to the electron beam, or of the spore at its center.

^b Carbon-coated (10-nm thickness).

^c Corrected for nonspecific background and for elemental background (<50 counts/min).

^d Microincineration for 1 hr at 600 C.

sample current followed the same patterns (Fig. 4B).

As a control, scans were made through spores that had been held for 20 min in boiling water so as to become depleted of Ca. A scan through such a spore of *B. cereus* resulted in a characteristic $C_{K\alpha}$ profile, but $Ca_{K\alpha}$ emissions were absent (Fig. 5A). A similar contrast was observed in a scanned vegetative cell which had been grown in the sporulation medium and washed in cold water (Fig. 5B).

Calcium location within intact spores. To obtain a direct and statistically significant comparison between the distribution of Ca and C, a linear differential scan was made in discontinuous mode through the center length of an intact *B. cereus* spore. The two sets of results were then normalized to enable direct comparison, i.e., the count at each step of the scan was divided by the respective maximum count. The normalized profiles for $Ca_{K\alpha}$ and $C_{K\alpha}$ were essentially identical (Fig. 6). If it is

assumed that X-ray intensity in first approximation is directly proportional to element concentration (7), Ca and C appeared to be distributed alike throughout the *B. cereus* spore.

The similar distribution of Ca and C in intact spores also was apparent from a comparison of the respective X-ray images, which were obtained by use of the multiline scanning mode of the microprobe. In Fig. 7 is shown a field of *B. megaterium* spores as seen in the secondary electron image (Fig. 7A), the $\text{Ca}_{K\alpha}$ image (Fig. 7B), and the $\text{C}_{K\alpha}$ image (Fig. 7C). The relatively less contrast in Fig. 7C resulted from coating the specimen with C.

A $\text{Ca}_{K\alpha}$ image of an intact *B. cereus* spore (Fig. 8), made with the highest instrumental magnification of $\times 20,000$, confirmed the above results. Apparently Ca was distributed throughout the spore but accumulated mostly in the center region, as judged with the limited resolution obtainable in an intact spore.

Calcium location within sectioned spores.

The spatial resolution obtainable by electron microprobe X-ray analysis can be increased considerably by use of sectioned specimens (7). Therefore, spores were fixed, dehydrated, embedded, and sectioned, with Ca omitted from the buffers used for fixing and washing. The possibility of Ca leakage from the spores during preparation for sectioning was examined by labeling spores with ^{45}Ca and measuring the possible loss of radioactivity after each preparational step (Table 2). Very little leakage of ^{45}Ca from the spores into the supernatant fluid was observed under the experimental conditions. Furthermore, $\text{Ca}_{K\alpha}$ was detected with the microprobe in individual spores after each of the preparational steps.

As it was impossible to discern a sectioned spore by means of the secondary electron image, transmission electron images were obtained from a section of the embedding mounted on a London finder grid to enable location of a given spore in the section. The grid was then transferred to the microprobe, and the spore was relocated by means of its sample current image.

Spores sectioned in the conventional manner and examined with the electron microprobe did not emit appreciable intensities of Ca-specific X rays (Table 3). Apparently, as suggested by Thomas (14, 15), Ca leaked out when a section of an embedding was collected from the microtome knife by flotation on water. As the embedding resins contained C predominantly, the $\text{C}_{K\alpha}$ intensities of the individual spore sections were only slightly greater than those of the background.

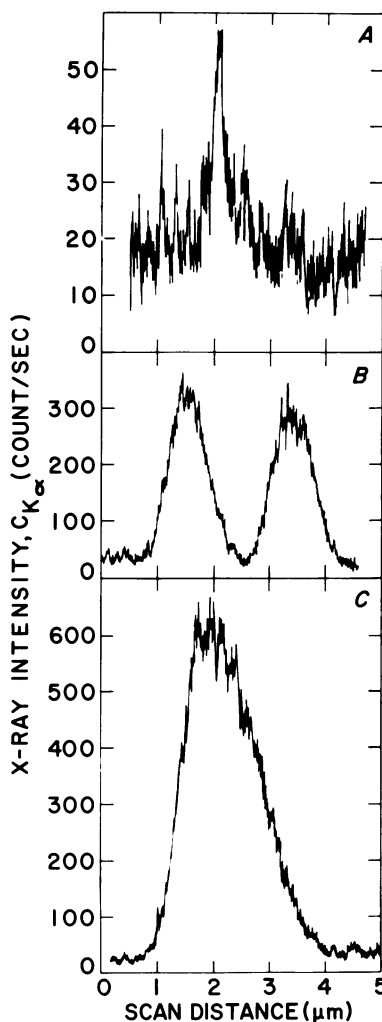


FIG. 3. $\text{C}_{K\alpha}$ profiles scanned linearly through a polystyrene latex sphere of diameter $0.365 \mu\text{m}$ (A), two of $1.17 \mu\text{m}$ (B), and one of $181 \mu\text{m}$ (C). The seemingly greater oscillations in Fig. 3A reflect the magnified scale of the ordinate. The specimens were carbon-coated on a quartz support. Microprobe specifications: 15-kv acceleration potential, 210-nm beam diameter, 20-namp sample current.

However, when a section of an embedding was collected directly from the edge of the knife and without contact with water, sectioned spores emitted Ca-specific X rays of relatively high intensity (Table 3).

Continuous linear scans were made through variously oriented sections of individual spores, which were recognized by their peaks of $\text{Ca}_{K\alpha}$ intensity (Fig. 9B). In comparison with a transmission electron image, this peak corresponded predominantly to the central region (Fig. 9A). Because of the absence of post-

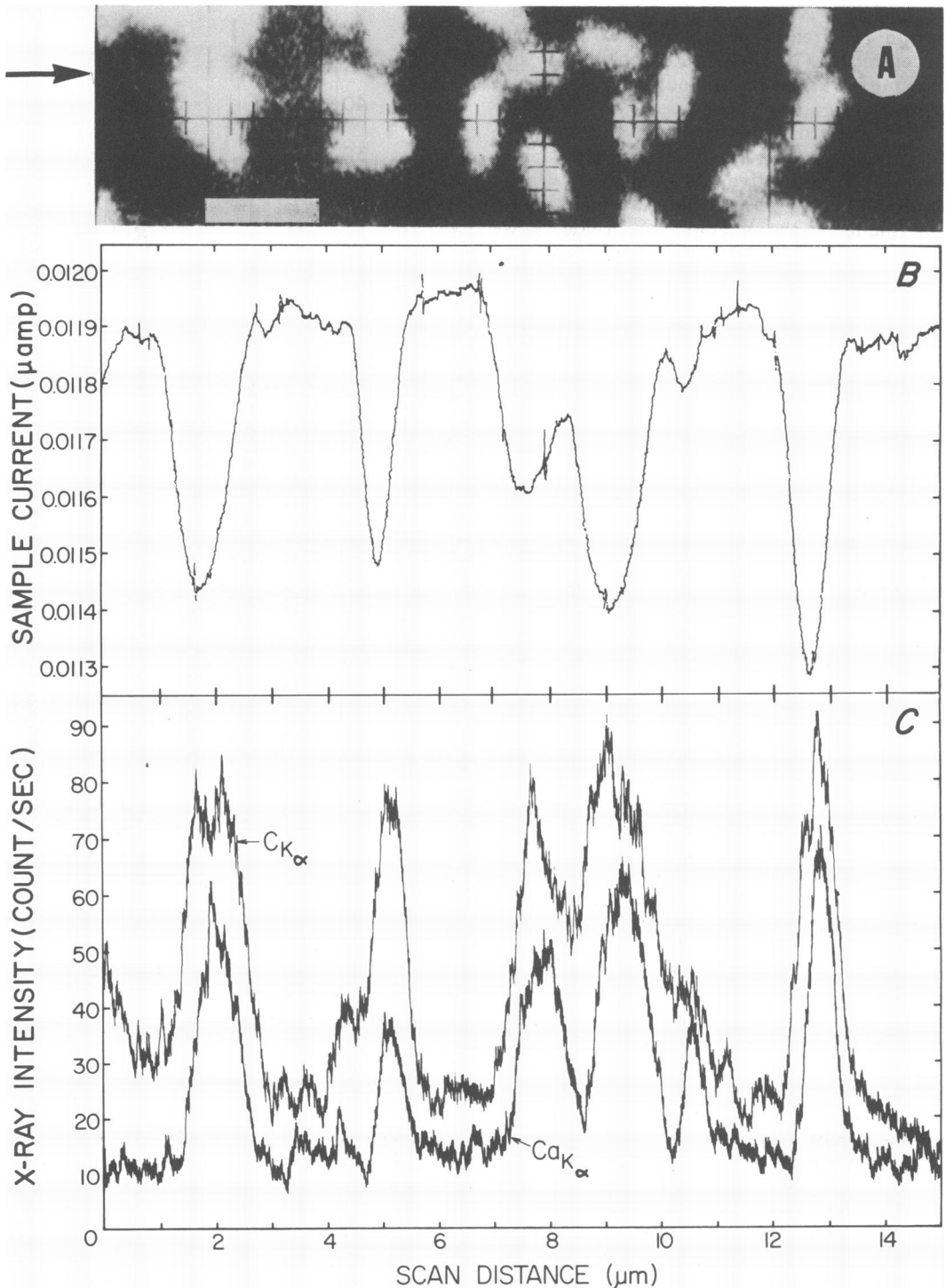


FIG. 4. Linear scan for $C_{K\alpha}$ and $Ca_{K\alpha}$ through a series of *B. cereus* spores (C), in comparison with the sample current variation (B) and the positioning of the spores seen in the corresponding secondary electron image (A). The relative position of the microprobe scan is indicated by the arrow. The specimen was carbon-coated on a quartz support. Microprobe specifications: 15-kv acceleration potential, 200-nm beam diameter, 12-namp sample current. Magnification bar, 2 nm.

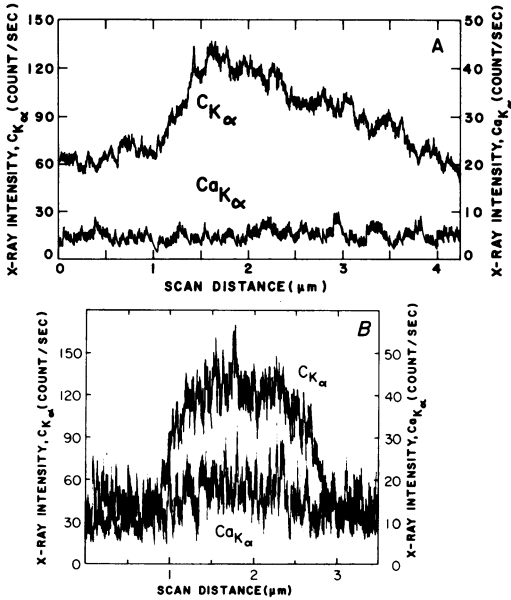


FIG. 5. Linear scan for $Ca_{K\alpha}$ and $C_{K\alpha}$ longitudinally (A) through an intact *B. cereus* spore after it was heated in water at 100 C for 20 min, and transversely (B) through an intact *B. cereus* vegetative cell. Microprobe specifications: 15-kv acceleration potential, 230-nm beam diameter, 20-namp sample current.

staining and the relative thickness of the sections (~ 200 nm), the electron images lacked contrast; nevertheless, the spore protoplast, coat, and exosporium were identifiable. A tangentially cut section of a spore with only the exosporium and a part of the coat (Fig. 9A, right) did not produce a significant $Ca_{K\alpha}$ peak (Fig. 9B, right) in the course of the same scan.

Finally, the embeddings were more thinly sectioned (~ 100 nm) to maximize spatial resolution and were mounted on a quartz slide to maximize X-ray intensity. An example of a $Ca_{K\alpha}$ profile for a longitudinally sectioned *B. megaterium* spore prepared in this way is shown in Fig. 10. It was evident that the $Ca_{K\alpha}$ occurred in the central peak predominantly, about 80% by graphical analysis. A secondary distribution of $Ca_{K\alpha}$ was evidenced as two shoulders or minor peaks. Other profiles of cross, tangential, and longitudinal sections of spores confirmed these findings.

Altogether, it was concluded from the results with sectioned spores as well as those with intact ones that Ca was distributed throughout the spore structure (cf. Fig. 1). Moreover, it was evident that the element was concentrated mainly in a central region corresponding to the spore protoplast.

DISCUSSION

An element present in as little as 0.01% of the cell dry weight can be detected with a microprobe (7). Assuming that a spore weighs about 1 pg (10^{-12} g), an element in the concentration range of fg (10^{-15} g) can be detected in a single spore. Detection and quantitative assay of a given element depends not only on the amount present, but also on the element in question (1, 7). The efficiency of the microprobe for the detection of $Ca_{K\alpha}$ is much greater than for that of $C_{K\alpha}$; e.g., much higher X-ray counts were obtained for Ca than for C in CaDPA, despite a greater amount of C.

The main problem in the use of the microprobe to locate Ca was spatial resolution. Intact spores behaved like "thick specimens," in Hall's (7) terminology. From application of Andersen's formulation (1), 70% of the incident electrons remained in the spore at an accelerating voltage of 15 kv, but some electrons may have been backscattered by the specimen support and thus increased the excited volume within the specimen. The smaller the excited volume, the better the spatial resolution (7); but the smaller the excited volume, the less the X-ray production. With application of Hall's (7) formulations to intact spores, the spatial resolution was in the order of 500 to 1,000 nm. With spores sectioned 100 to 200 nm in thickness, however, a spatial resolution of 100 to 200 nm was attained. This order of resolution proved adequate to locate Ca within a major structural region of a dormant spore.

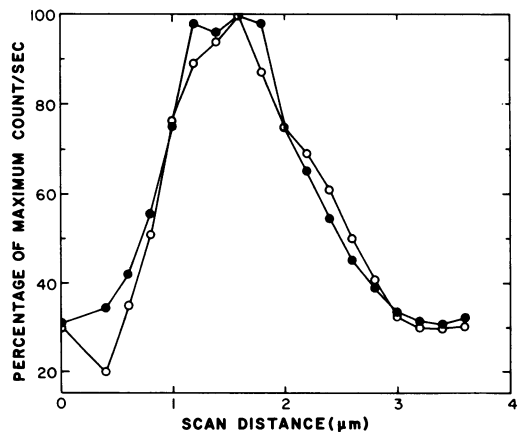


FIG. 6. Normalized profiles of $Ca_{K\alpha}$ (●) and $C_{K\alpha}$ (○) obtained by a discontinuous linear scan through the center length of an intact *B. cereus* spore. The maximum for $Ca_{K\alpha}$ was 150 counts/sec and for $C_{K\alpha}$, 140 counts/sec. Microprobe specifications: 14.5-kv acceleration potential, 200-nm beam diameter, 20-namp sample current.

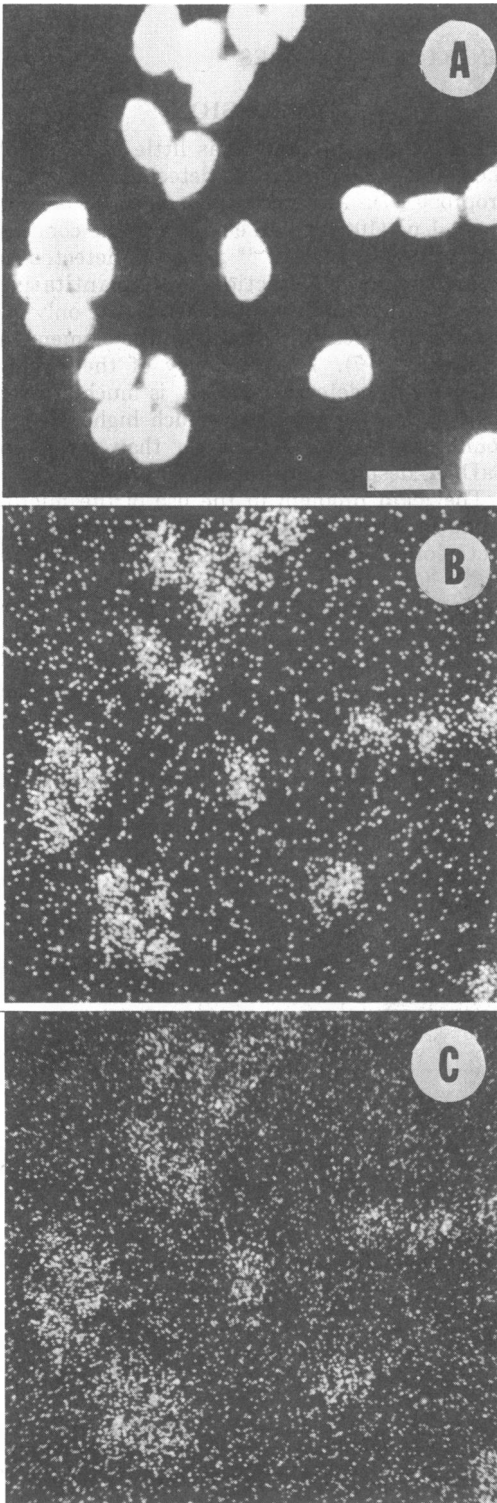


FIG. 7. Images of *B. megaterium* spores obtained with secondary electrons (A), $\text{Ca}_{K\alpha}$ X rays (B), and $\text{C}_{K\alpha}$ X rays (C). Total number of X-ray counts on scanned area ($320 \mu\text{m}^2$): $\text{Ca}_{K\alpha} = 10,334$, $\text{C}_{K\alpha} = 20,736$. Time of scan, 10 min. The specimen was coated with C and mounted on a quartz slide. Microprobe specifications: 30-kv acceleration potential, 100-nm beam diameter, 20-namp sample current. Magnification bar, $2 \mu\text{m}$.

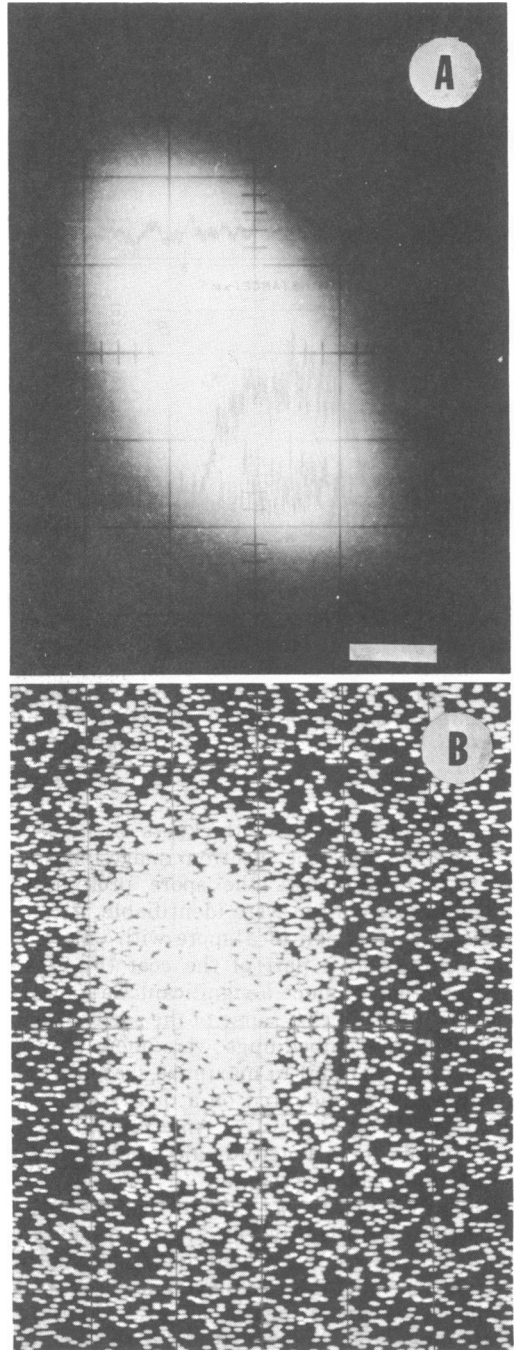


FIG. 8. Images at high magnification of a *B. cereus* spore obtained with secondary electrons (A) and $\text{Ca}_{K\alpha}$ X rays (B). Note that the area at the lower right pole of the electron image, which corresponded to extended exosporium, was not matched in the X-ray image. Total number of $\text{Ca}_{K\alpha}$ counts on scanned area ($20 \mu\text{m}^2$), 21,312; scan time, 10 min. The specimen was coated with carbon and mounted on a quartz slide. Microprobe specifications: 20-kv acceleration potential, 230-nm beam diameter, 15-namp sample current. Magnification bar, $0.5 \mu\text{m}$.

TABLE 2. ⁴⁵Ca content of spores during steps preparational for sectioning

Preparation step	Percentage of initial radioactivity ^a			
	<i>B. cereus</i> spores		<i>B. megaterium</i> spores	
	R-K ^b	Luft ^c	R-K ^b	Luft ^c
Aqueous suspension	100	100	100	100
Osmic acid fixation	97		98	
Glutaraldehyde fixation		96		95
Osmic acid postfixation		96		95
Uranyl acetate prestaining	96	95	97	95
Acetone dehydration ^d	95		96	
Ethanol dehydration ^d		95		95
Propylene oxide treatment		95		95
Vestopal embedding ^e	94		95	
Epon embedding ^e		94		94

^a Initial radioactivity of ⁴⁵C-labeled spores: 354,000 counts/min per 10 ml of *B. cereus* spore suspension and 325,000 counts/min per 10 ml of *B. megaterium* spore suspension. After each step, the spores were centrifuged and the radioactivity of the supernatant fluid was assayed.

^b Ryter-Kellenberger method (8).

^c Luft method (9).

^d Radioactivity after the final dehydration step.

^e Radioactivity after the first embedding step. The final embedding media were too viscous to be assayed.

TABLE 3. Static microprobe analysis^a of Ca_{Kα} and C_{Kα} intensities from *B. cereus* spore sections collected in the presence and absence of water

Method of collecting sections ^b	Location of electron beam	X-ray intensity (count/min) ^c	
		C _{Kα}	Ca _{Kα}
Direct removal	Embedding material	6,162	39
	Center of longitudinal spore section	7,258	342
	Center of spore cross section	6,864	165
Flotation on water	Embedding material	5,812	33
	Center of longitudinal spore section	6,115	34
	Center of spore cross section	6,098	32

^a Microprobe specifications: 30-kv acceleration potential, 100-nm beam diameter, 100-namp sample current.

^b Sections 200 nm thick (Peachey scale). Sections were mounted on London finder grids.

^c Without background correction.

Cells and spores consist mainly of elements of low atomic number such as carbon, hydrogen, oxygen, nitrogen, phosphorus, and sulfur, and smaller amounts of the heavier elements including calcium. Secondary electron images depend on the atomic numbers of cellular sur-

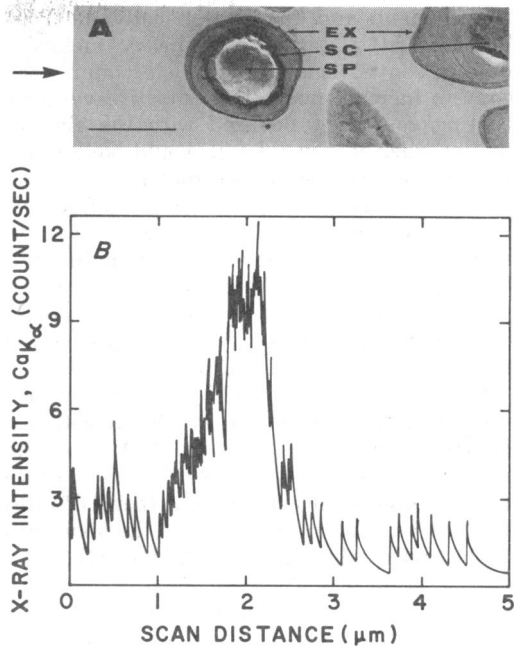


FIG. 9. Linear scan for Ca_{Kα} through a sectioned (200 nm) *B. cereus* spore mounted on a London finder grid (B), and the corresponding transmission electron microscope image (A). The relative position of the microprobe scan is indicated by the side arrow. Structural positions of the exosporium (EX), spore coat (SC) and protoplast (SP) are labeled. Microprobe specifications: 30-kv acceleration potential, 100-nm beam diameter, 20-namp sample current. Magnification bar, 1 μm.

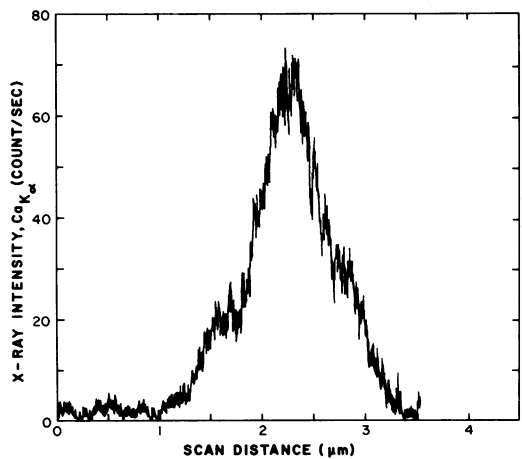


FIG. 10. Linear scan for Ca_{Kα} longitudinally through a sectioned (100 μm) *B. megaterium* spore mounted on a quartz slide. Microprobe specifications: 30-kv acceleration potential, 200-nm electron beam diameter, 19-namp sample current.

face elements and, therefore, usually are of low intensity (4). Coating with heavy metals is used in conventional scanning electron microscopy to increase image intensity. Heavy-metal coating could not be used with the electron microprobe, however, for it would have inhibited the penetration of electrons into the specimen and decreased the production of X rays. When the organic matrix of spores was destroyed by ashing, a much higher intensity of $\text{Ca}_{K\alpha}$ was produced. Thus, the spore matrix plays an important role in reducing the energy of the penetrating electrons and a possible role in absorbing the emitted X rays.

Elemental analysis with the microprobe, unfortunately, does not allow the detection of chemical compounds such as DPA. However, if the assumption is accepted that most of the DPA is associated with the Ca, then DPA also may be concentrated mainly in the spore proplast rather than in the cortex (see 11).

ACKNOWLEDGMENTS

This investigation was supported by a University Biomedical Sciences Research Support Grant from the National Institutes of Health to René Scherrer and by contract NONR-2587 from the Office of Naval Research to Philipp Gerhardt.

We acknowledge the helpful suggestions of H. Paul Rasmussen of the Department of Horticulture and especially the technical assistance and untiring patience of Vivion E. Shull of the Electron Microprobe Laboratory, both at Michigan State University.

LITERATURE CITED

1. Andersen, C. A. 1967. An introduction to the electron probe microanalyzer and its application to biochemistry. *Methods Biochem. Anal.* 15:147-270.
2. Beaman, T. C., H. S. Pankratz, and P. Gerhardt. 1972. Ultrastructure of the exosporium and underlying inclusions in spores of *Bacillus megaterium* strains. *J. Bacteriol.* 109:1198-1209.
3. Bearden, J. A. 1967. X-ray wavelengths. *Rev. Mod. Phys.* 31:78-124.
4. Birks, L. S. 1963. *Electron probe microanalysis*. Interscience Publishers, New York.
5. Carroll, K. G. 1967. Biological applications of the electron probe analyser, p. 69-79. In G. H. Bourne (ed.), *In vivo techniques in histology*. The Williams & Wilkins Co., Baltimore.
6. Gould, G. W., and A. Hurst (ed.). 1969. *The bacterial spore*. Academic Press Inc., London.
7. Hall, T. A. 1971. The microprobe assay of chemical elements, p. 157-275. In G. Oster (ed.), *Physical techniques in biological research*, vol. 1, part A, 2d ed. Academic Press Inc., New York.
8. Kellenberger, E., A. R. Ryter, and J. Séchaud. 1958. Electron microscope study of DNA-containing plasms. II. Vegetative and mature phage DNA as compared with normal bacterial nucleoids in different physiological states. *J. Biophys. Biochem. Cytol.* 4: 671-678.
9. Luft, J. M. 1961. Improvements in epoxy resin embedding methods. *J. Biophys. Biochem. Cytol.* 9:405-414.
10. Matz, L. L., T. C. Beaman, and P. Gerhardt. 1970. Chemical composition of exosporium from spores of *Bacillus cereus*. *J. Bacteriol.* 101:196-201.
11. Murrell, W. G., D. F. Ohye, and R. W. Gordon. 1969. Cytological and chemical structure of the spore, p. 1-19. In L. L. Campbell (ed.), *Spores IV*. American Society for Microbiology, Bethesda, Md.
12. Peachey, L. D. 1958. Thin sections. I. A study of section thickness and physical distortion produced during microtomy. *J. Biophys. Biochem. Cytol.* 4:233-242.
13. Strahs, G., and R. E. Dickerson. 1968. The crystal structure of calcium dipicolinate trihydrate (a bacterial spore metabolite). *Acta Cryst.* B24:571-578.
14. Thomas, R. S. 1964. Ultrastructural localization of mineral matter in bacterial spores by microincineration. *J. Cell Biol.* 23:113-133.
15. Thomas, R. S. 1969. Microincineration techniques for electron-microscopic localization of biological minerals. *Advan. Opt. Electron Microscopy* 3:99-154.